Faraday's law, Lenz's law, and conservation of energy

Lowell T. Wood,[a] Ray M. Rottmann, and Regina Barrera
Department of Physics, University of Houston, Houston, Texas 77204-5005

We describe an experiment in which the induced electromotive force in a coil caused by an accelerating magnet and the position of the moving magnet are measured as a function of the time. When the circuit is completed by adding an appropriate load resistor, a current that opposes the flux change is generated in the coil. This current causes a magnetic field in the coil which decreases the acceleration of the rising magnet, as is evident from the position versus time data. The circuit provides a direct observation of effects that are a consequence of Lenz's law. The energy dissipated by the resistance in the circuit is shown to equal the loss in mechanical energy of the system to within experimental error, thus demonstrating conservation of energy. Students in introductory physics courses have performed this experiment successfully. © *2004 American Association of Physics Teachers.*

I. INTRODUCTION

Many excellent demonstrations[1-5] and experiments[6-19] involving Faraday's law of electromagnetic induction have been discussed during the last several decades. In many of these experiments, relative motion between a conductor and a magnetic field occurs, and the subsequent induced electromotive force is studied as a function of the relative velocity, the number of turns in a coil, and the strength of the magnetic field.[7-15] Some experiments have used ac-driven primary coils and detected the induced emf in a secondary coil.[16,17] Eddy current damping and magnetic braking also have been studied. See Refs. 18 and 19, and references therein for further discussions of this aspect of Faraday's law.

We describe an experiment in which the induced emf in a coil caused by an accelerating magnet and the position of the moving magnet are measured simultaneously as a function of the time. From these data, we show how the magnetic forces caused by the induced current in the coil affect the motion of the magnet, and show that the energy dissipated in the circuit equals the mechanical energy loss in the system. Our experiment is conceptually similar to that of Fox and Reiber,[8] who allowed a moving coil on an air track to pass through a magnetic field and found experimentally that the kinetic energy loss of the air cart was equal to the Joule heating in the circuit. Our experiment differs from theirs in that we also record the position of the magnet as a function of time. These data give us access to features not discussed elsewhere.

In the experiment, a load resistor is connected to the coil. According to Lenz's law, the current induced in the coil opposes the change in the flux caused by the moving magnet. As the magnet's north pole enters the bottom end of the coil, the induced current sets up a magnetic field with its north pole opposing the north pole of the magnet, thereby reducing the flux increase and causing a repulsive force on the magnet. As the south pole of the magnet leaves the top end of the coil, the induced current opposes the flux decrease by causing a current whose magnetic field at the top of the coil is a north pole, thereby causing an attractive force on the magnet. The small ratio of the magnet length to the coil length causes the flux change to be small while the magnet is inside the coil, and the induced emf and current are correspondingly small.

The induced emf in the coil and the position of the magnet are collected by a computer as functions of time. Data taken with the load resistor in the circuit verify the discussion in the previous paragraph. For comparison, the coil is connected directly to the voltage probe with no load resistor in the circuit. Because of the high impedance of the voltage probe, the induced current and its resulting magnetic field are negligible. Therefore, the magnetic retarding forces do not measurably affect the motion of the magnet.

II. EXPERIMENTAL DETAILS

In our experiment, four small neodymium magnets (PASCO model EM-8648)[20] are combined to form a single magnet that acts as a single mass m of an Atwood's machine. A counterweight of mass M $(M > m)$ serves as the other mass. Figure 1 shows a photograph of the apparatus. A load resistor can be added to or removed from the circuit with a switch at the bottom of the apparatus. The pulley is a photogate/pulley system (PASCO model ME-6838). The top of the magnet is initially placed 0.10 m below the coil and released from rest. The magnet passes through the coil (secondary coil of PASCO's coil set, model SE-8653) and induces an emf in the coil. The emf is measured by an analog port of the PASCO 6510 Interface, and the photogate status is monitored by a digital port of the same interface.

The values for the relevant quantities used for these experiments are shown in Table I. The uncertainties reported are not statistical, but are determined by instrument resolution. (In a single 3-h laboratory, there is not sufficient time for statistical measurements.) When no uncertainty is reported, none was provided by the manufacturer. The uncertainties in these quantities are reported for completeness. They are not, however, the major contributers to the uncertainties in the final results, as we will discuss.

III. RESULTS AND ANALYSIS

Figure 2 shows a graph of the potential difference versus time for the voltage probe connected across the small load resistor R_S $(R_S = 8.51 \pm 0.01\,\Omega)$, the voltage probe connected across an intermediate load resistor R_I $(R_I = 74.9 \pm 0.1\,\Omega)$, and the voltage probe connected directly across the coil with no load resistor (approximating the open circuit voltage).
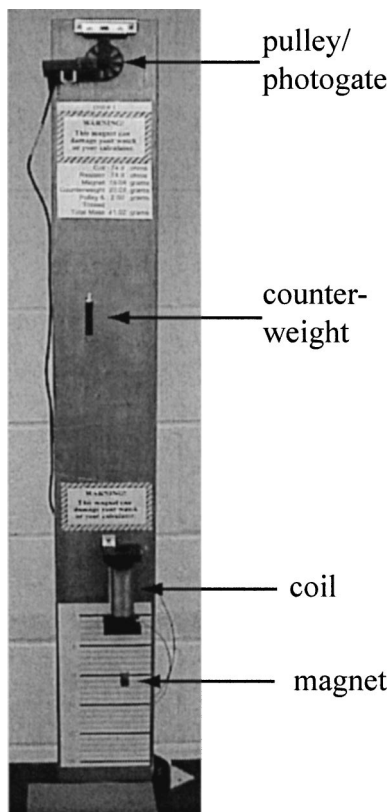
Fig. 1. Photograph of the apparatus. The magnet, coil, photogate/pulley system, and counterweight are shown. The load resistor is connected by a switch at the back of the apparatus.
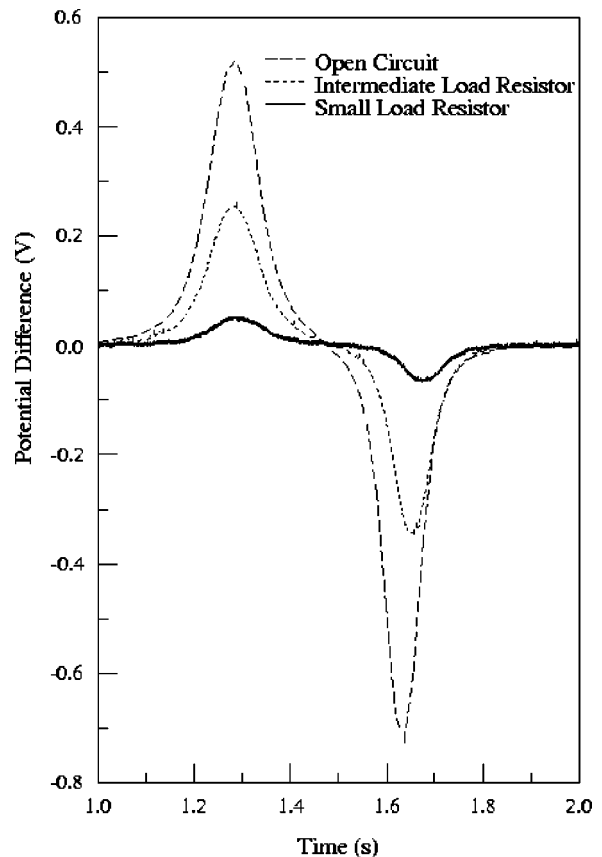

Fig. 2. Potential difference across the coil vs time for $R_S = 8.51 \, \Omega$, $R_I = 74.9 \, \Omega$, and open circuit. The increased time between the peaks as the load resistance decreases is clear. (The first peaks were aligned to illustrate clearly the time interval differences.)

Notice that the open circuit voltage is the largest, the voltage across R_S is the smallest, and the voltage across R_I lies between the two. In our apparatus, the magnitude of the induced emf as the magnet leaves the coil is greater than that when the magnet enters the coil because of the magnet's increased velocity. This greater velocity creates a more rapidly changing flux and a larger emf in accordance with Faraday's law.

Also notice that the time interval between the maximum voltage and the minimum voltage increases as the resistance decreases. This observation indicates that the average velocity for the magnet decreases as the load resistance decreases. The decrease in the average velocity indicates the presence of forces that oppose the motion. These forces are the repulsive force upon entering the coil and the attractive force upon exiting the coil, as discussed in Sec. I.

Table I. Summary of experimental parameters.

Mass of the magnet, m	19.04 ± 0.02 g
Mass of the counterweight, M	20.28 ± 0.02 g
Resistance of the coil, R_c	74.9 ± 0.1 Ω
Inductance of the coil, L_c	0.063 ± 0.001 H
Small load resistor, R_S	8.51 ± 0.01 Ω
Intermediate load resistor, R_I	74.9 ± 0.1 Ω
Pulley's moment of inertia, I_p	1.8×10^{-6} kg m^2
String's linear mass density, λ	$(7.0 \pm 0.1) \times 10^{-5}$ kg/m
Length of the string, L	1.300 ± 0.002 m
Diameter of the pulley, d	5.0 cm
Length of the magnet	2.00 ± 0.05 cm
Length of the coil	11.0 ± 0.1 cm

Figure 3 shows a graph of the total flux $N\Phi$ through the coil as a function of time, calculated by integrating the graph of the potential difference with time for the open circuit. Here N is the number of turns on the coil, and Φ is the flux through a single turn. Straight lines have been constructed to indicate the slope where the flux change is maximum and where it is minimum. The times for the maximum and minimum flux change are 1.28 and 1.64 s, respectively. As expected, these results correspond to the times for the maximum and minimum values of the potential difference in Fig. 2; the slopes are equal to the maximum and minimum potential difference values. Near the center of the coil, the flux varies slowly, and the corresponding induced emf is close to zero. As a consistency check, the integral of the emf over all time is zero to within the resolution of the equipment. Beyond these comments, many of the features of these curves depend on the specific geometries of the coil and the magnet.

Figure 4 shows a graph of current versus time for the load resistors R_S and R_I. (The current with no load resistor in the circuit is very nearly zero because the internal resistance of the voltmeter is $\sim 10^6 \, \Omega$.) The current is given by $I(t) = V_L / R_L$ (not V_L / R_c because of inductive effects), where V_L is the potential difference across the load resistor (or coil), and R_L is R_S or R_I. Again, note that the time interval between the maximum current and the minimum current increases as the resistance decreases.

The observation of the time interval change caused by the retarding forces on the magnet leads naturally to a consider-
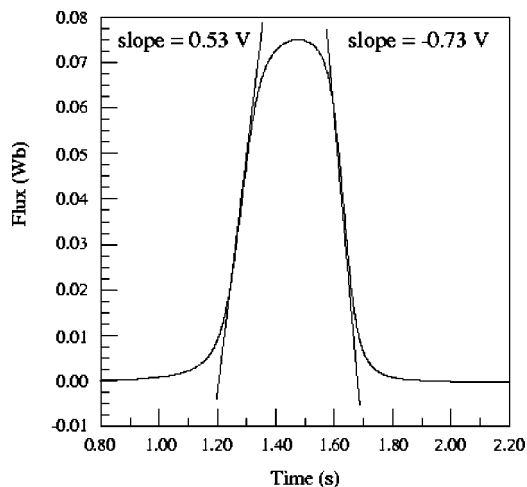
Fig. 3. Flux vs time for the open circuit emf. The points where the maximum and minimum slopes occur have straight lines drawn through them to accentuate the slope differences. The flatter region of the peak corresponds to a small induced emf when the magnet is near the center of the coil.

Fig. 5. Velocity squared vs position. Closed triangles represent the open circuit case, open circles represent $R_I = 74.9\ \Omega$, and closed circles represent $R_S = 8.51\ \Omega$. The kinks at 0.10 and 0.22 m correspond to the positions where the magnet enters the coil and where it leaves the coil. Note that for the closed circles, the acceleration and velocity decrease as the magnet leaves the coil. The solid lines are least-squares fitted straight lines over the range $y = 0.29$ m to $y = 0.50$ m. The slopes of the fitted lines are (0.548 $\pm$0.004) m/s² when R_S is in the circuit, (0.548$\pm$0.003) m/s² when R_I is in the circuit, and (0.548$\pm$0.006) m/s² for the open circuit.

ation of the kinetics of the system and energy changes in the system. The retarding forces on the magnet cause the kinetic energy to be less than that with no load resistor present. This loss in kinetic energy must be consistent with the energy dissipated in the coil and in the load resistor. Because we wish to consider kinetic energy losses and forces on the magnet, we choose to plot the velocity squared versus the displacement, that is, $v^2 = v_0^2 + 2a\Delta y$, where v is the velocity, v_0 is the initial velocity, a is the acceleration, and Δy is the
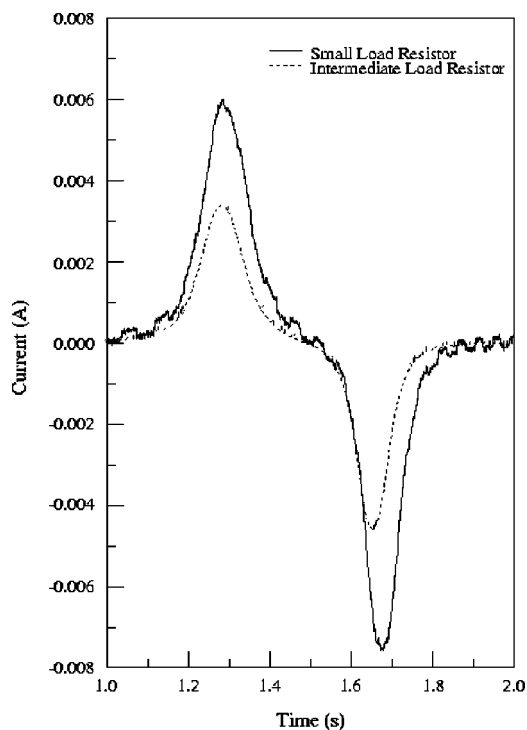
displacement. The slope of this line represents twice the acceleration, which is directly proportional to the force on the magnet.

Figure 5 shows a graph of v^2 vs Δy with no load resistor, an intermediate load resistor R_I, and a small load resistor R_S. With no load resistor, the induced current in the coil is very small due to the large resistance of the voltage probe. The magnetic field is so small that there is no detectable change in the acceleration of the magnet as it passes through the coil. For the intermediate load resistor, the induced current in the coil produces a larger magnetic field that opposes the flux change, thereby producing a repulsive force that measurably decreases the acceleration of the magnet as it enters the coil. While the magnet is inside the coil, the flux change is small, almost no current exists, and the magnet resumes its nearly constant acceleration. As the magnet leaves the coil, the induced current again opposes the flux change, this time resulting in an attractive force that again decreases the acceleration of the magnet. The two kinks in Fig. 5 (open circles and closed circles) at $x = 0.1$ m and $x = 0.22$ m correspond to the magnet entering the coil and leaving the coil. While the magnet is far from the coil on either side, no significant induced currents or forces exist, and the system behaves as a conventional Atwood's machine with nearly constant acceleration.

For the circuit using R_S, the situation is very much the same as for the circuit using R_I, except that the smaller value for the load resistor results in a larger induced current, larger repulsive and attractive forces, and a greater change in

Fig. 4. Current vs time for $R_S = 8.51\ \Omega$ and $R_I = 74.9\ \Omega$. Note that the magnitude of the current for the smaller load resistor is the larger of the two. (The first peaks were aligned to illustrate clearly the time interval differences.)
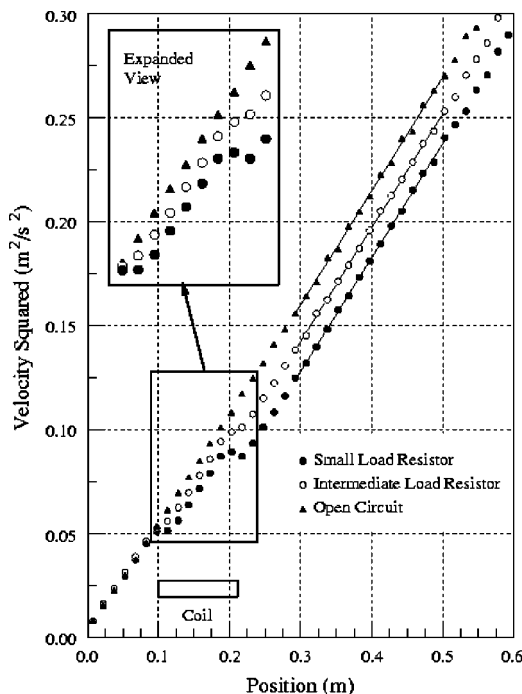
the acceleration. In fact, for R_S (closed circles), the second kink ($x = 0.22$ m) clearly shows that the retarding forces are larger in magnitude than the accelerating forces on the Atwood machine, and that they produce a negative acceleration for a short distance, that is, the velocity decreases, reaches a minimum, and then increases within a short distance. (The expanded view in Fig. 5 shows this feature more clearly.) These kinks are clear evidence that forces arising from the induced currents cause measurable effects on the motion of the magnet.

Our analysis of energy conservation relies on the fact that the apparatus behaves as a ordinary Atwood machine when no load resistor is in the circuit. When a load resistor is in the circuit, the retarding forces discussed earlier decrease the kinetic energy of the system, and the currents generated give rise to Joule heating in the load resistor and in the coil. If frictional losses and potential energy changes are the same for each case, the kinetic energy differences with and without a load resistor can be simply related to the energy dissipated by Joule heating.

To analyze energy conservation quantitatively, we use the work-energy theorem, which states that

$$W = \Delta U + \Delta K, \tag{1}$$

where W is the work done by nonconservative forces, U is the gravitational potential energy, and K is the kinetic energy. The most dominant nonconservative forces in our experiment are friction in the pulley bearing and dissipative forces that ultimately convert mechanical energy into Joule heating. Therefore, the work-energy theorem may be written as

$$W_d(R_L) + W_f = \Delta U + K(R_L), \tag{2}$$

where $W_d(R_L)$ is the work done by the material dissipative force, W_f is the work done by the frictional force in the pulley bearing, ΔU is the change in potential energy, and $K(R_L)$ is the change in kinetic energy. (The initial kinetic energy for each data set is zero.) Note that W_d and K are functions of R_L, which can be R_S, R_I, or an open circuit. Our experiment is carried out such that W_f and ΔU are the same whether or not the load resistor is in the circuit. Therefore, if we subtract Eq. (2) without a load resistor from Eq. (2) with a load resistor present, we obtain

$$W_d(R_L) = K(R_L) - K(0), \tag{3}$$

where $K(0)$ is the change in kinetic energy with no load resistor in the circuit and $W_d(0)$ is approximately zero.

The kinetic energy of the system is given by

$$K = (1/2)(M+m)\nu^2 + (1/2)I_p\omega_p^2 + (1/2)\lambda L\nu^2. \tag{4}$$

Here ν is the velocity of the magnet after traveling a distance Δy, L is the length of the connecting string, I_p is the moment of inertia of the pulley, λ is the string's linear mass density, and ω_p is the angular velocity of the pulley. Only ν (and ω_p through its dependence on ν) will vary with a change in the load resistance. The first term in Eq. (4) is the kinetic energy of the counterweight and magnet, the second term is the kinetic energy of the pulley, and the third term is the kinetic energy of the connecting string.

For each data set, the magnet is released from rest 0.1 m below the coil and is tracked through the same distance (~ 0.50 m). Therefore, the change in the gravitational potential energy is the same whether a load resistor is present or not provided that Δy is the same for each case. The fitted
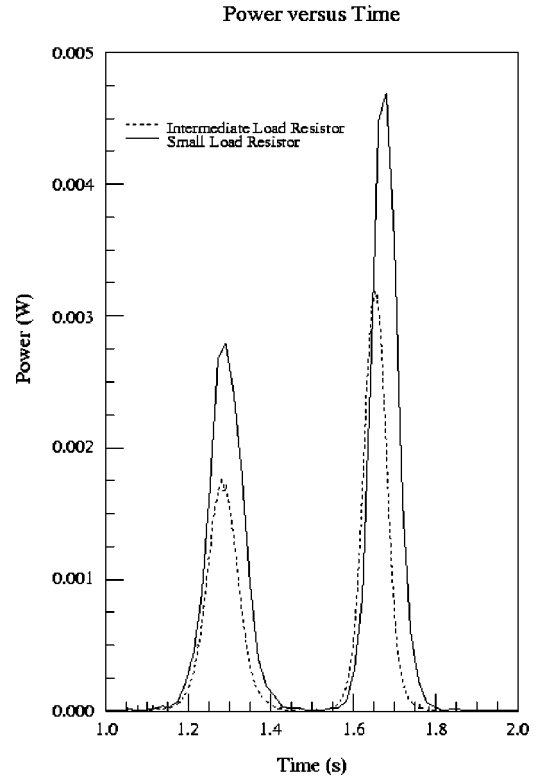

Fig. 6. Power vs time for $R_S = 8.51\,\Omega$ and $R_I = 74.9\,\Omega$. The energy dissipated in the circuit is calculated by numerically integrating each of these two curves. (The first peaks were aligned to illustrate clearly the time interval differences.)

lines in Fig. 5 all cover the same distance from 0.29 m to 0.50 m, so $\Delta y = 0.21$ m for each data set. The slopes of the fitted lines in Fig. 5 are (0.548 ± 0.004) m/s^2 when R_S is in the circuit, (0.548 ± 0.003) m/s^2 when R_I is in the circuit, and (0.548 ± 0.006) m/s^2 for the open circuit. (The uncertainties in the slopes are those reported by the fitting program.) This level of agreement means that the velocity dependence of the frictional forces is negligible for this experiment and that the frictional forces overall are approximately the same (about one-third the value of the resistive losses for R_S as determined from a separate calculation).

If we substitute numbers into Eq. (4) and use these results in Eq. (3), the result for $W_d(R_L)$ from the kinetic energy difference is $W_d(R_L) = -(2.11 \times 10^{-2})[\nu(0)^2 - \nu(R_L)^2]$, where $\nu(0)$ is the velocity with no load resistor in the circuit and $\nu(R_L)$ is the velocity with a load resistor. By averaging the point-by-point differences in the actual data between 0.29 m and 0.50 m in Fig. 5, the kinetic energy difference when R_S is in the circuit is $(-6.76 \pm 0.44) \times 10^{-4}$ J, whereas when R_I is in the circuit, the kinetic energy difference is $(-3.73 \pm 0.34) \times 10^{-4}$ J.

To obtain the energy loss from Joule heating, we first calculate $P(t) = i^2(t)(R_L + R_c)$. Recall that the current $i(t) = V_L/R_L$. Figure 6 shows the power dissipated in each circuit as a function of time. As expected, the larger power dissipation in the entire circuit occurs for the smaller of the two load resistors because the current is nearly doubled, whereas the resistance is approximately halved. (Again, the longer time between the peaks for the larger current is evident.) The total dissipated energy, the integral of $P(t)$ over t,

Table II. Experimental results.

Load resistance	Kinetic energy loss	Electrical energy dissipated
8.51±0.01 Ω	$(6.76\pm0.44)\times10^{-4}$ J	$(6.78\pm0.17)\times10^{-4}$ J
74.9 ±0.1 Ω	$(3.73\pm0.34)\times10^{-4}$ J	$(3.91\pm0.01)\times10^{-4}$ J

is calculated numerically using PSI-Plot.[21] For the small load resistor, the total dissipated energy is $(6.78\pm0.17)\times10^{-4}$ J, and for the intermediate load resistor, the total dissipated energy is $(3.91\pm0.01)\times10^{-4}$ J. The uncertainties in the energy dissipated for each load resistor are calculated by determining the average fluctuation in the potential difference when the magnet is not near the coil. (These fluctuations are too small to be observed in Fig. 2.) The first 0.5 s is used for this purpose, and the average fluctuation of ±0.0016 V is observed to be approximately constant for all values of the potential difference. The current, power, and energy for each load resistor is recalculated using the potential difference in Fig. 2 with 0.0016 V added to or subtracted from those values. The average energy differences are reported as the uncertainties in Table II. The smaller uncertainty for the intermediate load resistor results from its larger potential difference, which, for a constant fluctuation, yields a smaller uncertainty.

IV. DISCUSSION AND CONCLUSION

We have presented a straightforward experiment that demonstrates qualitatively and quantitatively several aspects of Faraday's law of electromagnetic induction and Lenz's law, while also verifying conservation of energy. Specifically, several features are clear. (1) The magnitude of the induced emf increases as the magnet leaves the coil because the velocity of the magnet is larger, thereby producing larger flux changes per unit time. (2) The force produced by the interaction of the induced magnetic field in the coil with the magnet is large enough to decrease the magnet's acceleration and, in at least one case, to decrease the magnet's velocity. (3) The time required for the magnet to traverse the coil increases as the load resistance is decreased because the average velocity is reduced for the latter case. The increase in the separation of the peaks in Figs. 2, 4, and 6 shows this effect. (4) The loss in mechanical energy equals the energy dissipated as Joule heating in the circuit, clearly demonstrating energy conservation in this process.

We have used this experiment for students in our algebra- and calculus-based introductory laboratories, but the experiment can easily be adapted for more advanced students. For example, students in an advanced laboratory could consider additional aspects of this experiment such as calculating the magnetic field along the axis of the solenoid and determining the magnetic force acting on the magnet. If somewhat higher position resolution were used, a more detailed analysis of the accelerations and forces could be performed and compared to the calculated forces. We note that this experiment resembles the standard example of pulling a loop of wire through a magnetic field at constant velocity, where it is shown that the power dissipated in the resistor is equal to the mechanical power required to pull the loop through the region of the magnetic field.[22] In our experiment, an otherwise nearly constant acceleration is changed by the magnet moving through a coil as induced currents develop, creating forces that oppose the magnet's motion and decrease its acceleration.

a)Electronic mail: ltwood@uh.edu

[1] R. Sutton, *Demonstration Experiments in Physics* (McGraw–Hill, New York, 1938), pp. 339–344.

[2] H. Lemon and F. Marshall, *The Demonstration Laboratory of Physics at the University of Chicago* (University of Chicago Press, Chicago, 1939), pp. 51–52.

[3] H. Meiners, *Physics Demonstration Experiments* (Ronald, New York, 1970), Vol. 2, pp. 932–948.

[4] R. Sankovich, "Faraday's law demonstration," Am. J. Phys. **53**, 89 (1985).

[5] R. Ehrlich, *Turning the World Inside Out* (Princeton U.P., Princeton, 1990), p. 165.

[6] J. A. Fox, "An experiment on velocity and induced emf," Am. J. Phys. **33**, 408–410 (1965).

[7] J. Fredrickson and L. Moreland, "Electromagnetic induction: A computer-assisted experiment," Am. J. Phys. **40**, 1202–1205 (1972).

[8] J. N. Fox and D. G. Reiber, "Magnetic induction and the linear air track," Am. J. Phys. **41**, 75–77 (1973).

[9] L. J. Reed, "Magnetic induction and the linear air track," Am. J. Phys. **43**, 555–556 (1975).

[10] P. Rochon and N. Gauthier, "Induction transducer for recording the velocity of a glider on an air track," Am. J. Phys. **50**, 84–85 (1982).

[11] R. C. Nicklin, "Faraday's law—Quantitative experiments," Am. J. Phys. **54**, 422–428 (1986).

[12] J. A. Manzanares, J. Bisquert, G. Garcia-Belmonte, and M. Fernandez-Alonso, "An experiment on magnetic induction pulses," Am. J. Phys. **62**, 702–706 (1994).

[13] P. Carpena, "Velocity measurements through magnetic induction," Am. J. Phys. **65**, 135–140 (1997).

[14] A. Singh, Y. N. Mohapatra, and S. Kumar, "Electromagnetic induction and damping: Quantitative experiments using a PC interface," Am. J. Phys. **70**, 424–427 (2002).

[15] R. Kingman, S. C. Rowland, and S. Popescu, "An experimental observation of Faraday's law of induction," Am. J. Phys. **70**, 595–598 (2002).

[16] C. C. Jones, "Faraday's law apparatus for the freshmen laboratory," Am. J. Phys. **55**, 1148–1150 (1987).

[17] J. Barbero, J. A. Manzanares, and S. Mafe, "Induced emf in a solenoid: A simple quantitative verification of Faraday's law," Phys. Educ. **29**, 102–105 (1994).

[18] C. S. MacLatchy, P. Backman, and L. Bogan, "A quantitative magnetic breaking experiment," Am. J. Phys. **61**, 1096–1101 (1993).

[19] K. D. Hahn, E. M. Johnson, A. Brokken, and S. Baldwin, "Eddy current damping of a magnet moving through a pipe," Am. J. Phys. **66**, 1066–1076 (1998).

[20] We used apparatus manufactured by PASCO Scientific, but other vendors make similar items.

[21] PSI-Plot is a registered trademark of Poly Software International.

[22] D. Halliday, R. Resnick, and K. Krane, *Physics* (Wiley, New York, 1992), 4th ed., Vol. 2 extended, pp. 787–789.